Environ Earth Sci (2016) 75:876
DOI 10.1007/s12665-016-5590-9

ORIGINAL ARTICLE

Relationship between sub-cloud secondary evaporation and stable isotope in precipitation in different regions of China

Guo-feng Zhu[1,2] · Jia-fang Li[1] · Pei-ji Shi[1] · Yuan-qing He[2] · Ao Cai[3] · Hua-li Tong[1] · Yuan-feng Liu[1] · Ling Yang[1]

Received: 8 June 2015 / Accepted: 25 March 2016

Abstract Falling to the ground from the bottom of clouds, rain experiences evaporation process, which has a very important role for accurate analysis of isotope water cycle information and the improvement of isotope hydrology system. As an integral part of the water cycle research, this evaporation process gradually arise people's attention. Based on the precipitation isotope data obtained from GNIP site or some observation and literature, the existence and influence factors of secondary evaporation effects are studied in different regions of China. The study areas are divided into four regions (northwest arid region, southeast monsoon region, southwest monsoon region, and the Tibetan Plateau region), and the results show that the four regions exist the secondary evaporation effect. The seasonal change is obvious in the northwest arid areas and the north of the southeast monsoon region, and it is strong in summer and weak in winter. In the northwest arid areas and the monsoon region in dry season, it has a strong secondary evaporation effect when rainfall is less, and there is no significant correlation between monsoon rainfall and the secondary evaporation effect during the rainy season. The relationship between temperature and secondary evaporation is not obvious in the north of the southeast monsoon region during rainy season, while the sub-cloud secondary evaporation is more intense in high temperatures in other areas. In addition to the northwest arid region and north of the southeast monsoon region in the dry season, the relationship between the secondary evaporation effect and the relative humidity is significant. In high relative humidity, the secondary evaporation effect gradually weakens with the increase in the relative humidity.

Keywords Stable isotope · Secondary evaporation effect · Precipitation · Relative humidity

Introduction

As unique tracers and indicators of environmental conditions (Araguás et al. 1998; Dansgaard 1953, 1964), stable isotope technique has been widely applied in hydrology, climatology, ecology, and other areas of research, providing important information on the study of the mechanism of atmospheric circulation patterns and water cycle (Friedman et al. 1964; Merlivat and Jouzel 1979; Yurtsever and Gat 1981; Rozanski et al. 1993; Zhang and Yao 1994; Hoffman et al. 2000; Bowen and Wilkinson 2002) and giving solutions to discover the origin and formation of different water bodies, to study the circulation movement and approaches, and to estimate circulation rate and other scientific issues (Sengupta and Sarkar 2006; Yamanaka et al. 2007). Nevertheless, we also find that with the advance of research, the classical theory in the field of isotope hydrology: Rayleigh fractionation model still exists some minor deficiencies in practice, for example, the model can only demonstrate how to simulate air mass in the process of running by fractionation coefficient or decrease in the water vapor content in the air under the influence of the factors, such

✉ Jia-fang Li
tlijiafang@163.com

[1] College of Geography and Environmental Sciences, Northwest Normal University, Lanzhou 730070, China

[2] State Key Laboratory of Cryosphere Sciences, Cold and Arid Regions Environmental and Engineering Research Institute, Chinese Academy of Sciences, Lanzhou 730070, China

[3] College of Resources and Environment, Lanzhou University, Lanzhou 730070, China

Published online: 11 May 2016

as isotopic values change, without considering the external water supplies and the secondary evaporation during raindrops fall to the ground from the bottom of the cloud (Araguás et al. 2000; Gat 2000; Ma et al. 2013; Kreutz et al. 2003; Peng et al. 2004; Tian et al. 2007). Evaporation of water is the comprehensive result of equilibrium fractionation and dynamic fractionation (Tian et al. 2000). As an important part in natural water cycle, it constitutes the hydrological cycle of water on the earth with condensation, landing, and runoff. It is the most direct factor affected by the climate change in the process of water cycle (Wang et al. 2010), which has a very positive meaning to the study of global and local water cycle. Therefore, the secondary evaporation effect under clouds should be considered in studies using isotopic approaches (Gat and Matsui 1991; Gat et al. 1994; Peng et al. 2007, 2010; Froehlich et al. 2008; Liu et al. 2008a; Meng and Liu 2010; Kong et al. 2013; Chen et al. 2015).

The sub-cloud secondary evaporation refers to the process of evaporation when precipitation falls from the bottom of the clouds to the ground. Under unsaturated vapor pressure conditions, when raindrops fall, some rain evaporates accompanied by isotope fractionation (Dansgaard et al. 1964), and this has some impacts on isotopic composition of precipitation as well as atmospheric water vapor. Due to the different evaporation rates, in the process of evaporation, light isotope preferentially evaporates, while heavy isotope enriches (Miyake et al. 1968; Stewart 1975; Yapp 1982; Jouzel and Merlivat 1984). In addition, affected by the sub-cloud secondary evaporation, the precipitation will show d-excess dilution [d-excess $= \delta^{2}$-H $- 8\delta^{18}$O (Dansgaard 1964)] (Liu et al. 2008b; Kress et al. 2010; Steen-Larsen et al. 2011). Furthermore, under the influence of the isotope fractionation effect, the slope and intercept of the meteoric water line (MWL) equation become smaller (Dansgaard et al. 1964; Stewart 1975). Therefore, the change of the δD, δ^{18}O, slope, and the d-excess value in precipitation can be used as a powerful tool to predict the existence of the secondary evaporation effectively as well as to study the influence factors of secondary evaporation effect and influence degree (Peng et al. 2007; Liu et al. 2008a; Meng and Liu 2010; Ma et al. 2012; Zhang et al. 2012).

Stewart (Stewart 1975) calculated the ratio of different regions about secondary evaporation under laboratory conditions relying on the droplet evaporation model. Zhang et al. (1998) showed that the δ value enriches as the rain drops of distance increase in unsaturated atmospheric, and the δ value increases more obvious in drying air condition, which may be affected by secondary evaporation. Kendall (Kendall and Coplen 2001) made a conclusion of which the slopes of river less than 6.0 may be caused by precipitation's evaporation in semi-arid regions of the western USA. Pang et al. (2011) discovered that d-excess had a high correlation with temperature in Tianshan, which was a new evidence to explain interaction between secondary evaporation and moisture recirculation in arid regions. In 2008, Froehlich (Froehlich et al. 2008) studied the influence of second evaporation to d-excess of precipitation in the Alps based on Stewart's experimental conclusion, and he found that when raindrops evaporation capacity within 7 %, evaporation increased by 1 % with d-excess reduced about 1 ‰. This conclusion makes it possible to universal quantitative research, and to study relationship between secondary evaporation and d-excess. The model also has application cases in other area (Kong et al. 2013) and limited to calculate complexity; more studies directly use the research of Froehlich to inversion (Peng et al. 2010; Ma et al. 2014; Chen et al. 2015). However, the application of this method in drought environment (raindrops evaporation capacity may be greater than 7 %) is still limited, and under the condition of high evaporation and low humidity, whether the conclusion can keep linear relationship needs further validation (Wang 2015). In addition, whether there is sub-cloud secondary evaporation in different climate type regions still remains to be proved. If there is the secondary evaporation effect in some area, their local characteristic and difference of intensity level, the internal mechanism between secondary evaporation and stable isotopes, especially the meteorological forcing for the different study region, all need further investigation. Based on precipitation samples and related meteorological parameters collected from the four study regions, the relationship between below-cloud secondary evaporation and stable isotope in precipitation is analyzed in this study.

Materials and methods

Stable isotope data of precipitation come from two different ways. One data get from Global Network of Isotopes in Precipitation (GNIP) established by the International Atomic Energy Agency (IAEA) and the World Meteorological Organization (WMO) in 1961. In this network, the isotope compositions of precipitation from current 379 active worldwide stations are reported based on amount-weighted monthly average δ^{2}H and δ^{18}O values (e.g., Rozanski et al. 1993; Gourcy et al. 2005). Data from GNIP sites are selected more than a period of 5 years, so it has good stability and continuity. The other comes from the observation or the literature (Fig. 1) (Liu et al. 2008a; Yu et al. 2006, 2009; Zhang and Yao 1996; Tian et al. 2001; Li et al. 2013; Chen et al. 2015). The following problems should be paid attention to in the process of sampling. To reduce the influence of water

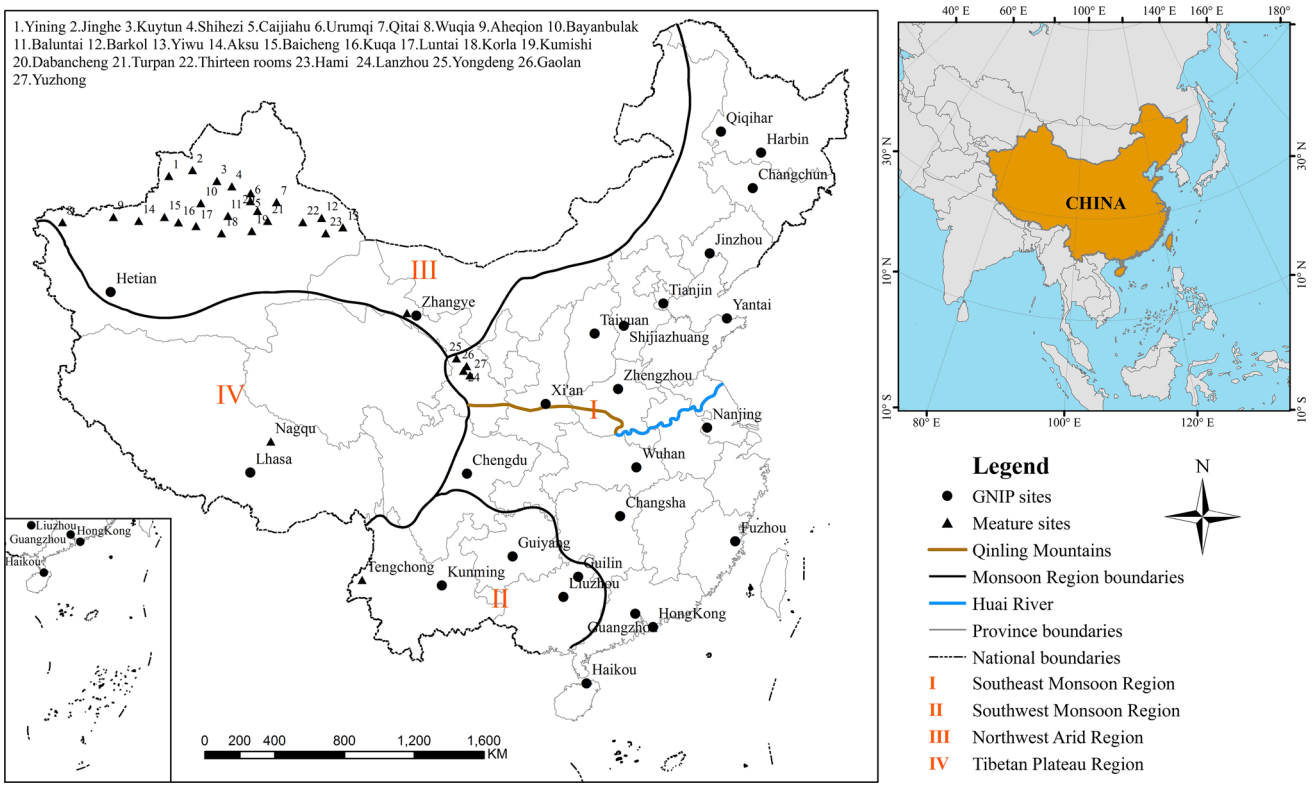

Fig. 1 Locations of study area and sampling stations

evaporation to sample, the water samples were collected as soon as each precipitation process was over. If precipitation was liquid, the sample was filled into plastic bottles, and then the capped bottles were sealed using tapes. For solid precipitation (snow), the sample was packed into an airtight plastic bag, and then put into a bottle after it melted completely. The surface air temperature, precipitation amount, atmospheric water vapor pressure, and relative humidity were recorded at the initial and end time of each precipitation event. All samples were kept frozen. Samples were removed in batches to thaw and were melted naturally at room temperature before they were analyzed for stable isotopes. The detailed information of observation data can be seen in Table 1. The division of the southeast monsoon region in north and south areas is on the basis of Qinling Mountains—Huai River line. The measurement results relatively contrasting to the 1000 difference (i.e., international unified by measured isotope ratios and standard samples of the same isotope of an element relative to 1000 difference as a measure) of standard mean ocean water's (standard mean ocean water, SMOW) are expressed as the following form:

$$\delta^{18}O\,(‰) = (R_S/R_{\text{smow}} - 1) \times 1000 \quad (1)$$

where R_s represents the ratio of precipitation in $^{18}O/^{16}O$ and R_{smow} is the ratio of $^{18}O/^{16}O$ in SMOW.

Hydrogen and oxygen stable isotopes in precipitation weighted average are as follows:

$$\delta_{(w)} = \sum P_i\delta_i / \sum P_i \quad (2)$$

where $\delta_{(W)}$ represents precipitation weighted average value, P_i is the precipitation in the ith month, and δ_i is the stable isotope ratio in the ith month.

In addition to the isotopic data, this study selects meteorological data of 32 sites in the study area provided by China Meteorological Data Sharing Service System (CMDSSS) complementing the lack of measured values for each site in different years of the average monthly precipitation, monthly temperature, vapor pressure, and the relative humidity.

Results and analysis

Impact factors and existence of sub-cloud secondary evaporation

Craig found that there is a linear relationship between δD and $\delta^{18}O$ in precipitation during the research in 1961, this relationship is called global meteoric water line (GMWL) (Craig 1961). The slope of GMWL reflects comparison of the fractionation rates of two kinds of stable isotope: D and ^{18}O, and the constant term indicates the degree of deviation

Table 1 Observation data information (a) locations of data, (b) sample information of data

Regions	Sites	Geographic information
(a)		
Tibetan Plateau region	Nagqu	Nagqu (31.48°N, 92.07°E, 4507 m)
Northwest arid region	Zhangye	Zhangye (39.04°N, 100.13°E)
	Lanzhou and surrounding area*	Lanzhou (36.10°N, 103.73°E, 1548.0 m)
		Yongdeng (36.75°N, 103.25°E, 2118.8 m); Gaolan (36.35°N, 103.93°E, 1668.5 m); Yuzhong (35.87°N, 104.15°E, 1874.4 m)
	Tianshan area	The northern slope of Tianshan Mountains: Yining (43.95°N, 81.33°E); Jinghe (44.62°N, 82.9°E); kuytun (44.4°N, 84.87°E); Shihezi (44.32°N, 86.05°E);
		Caijiahu (44.2°N, 87.53°E); Urumqi (43.78°N, 87.65°E); Qitai (44.02°N, 89.57°E)
		Tianshan Mountains: Wuqia (39.72°N, 75.25°E); Aheqion (40.93°N, 78.45°E); Bayanbulak (43.03°N, 84.15°E); Baluntai (42.73°N, 86.3°E); Barkol (43.6°N, 93.05°E); Yiwu (43.27°N, 94.7°E)
		The southern slope of Tianshan Mountain: Aksu (41.02°N, 80.23°E); Baicheng (41.78°N, 81.9°E); Kuqa (41.72°N, 82.97°E); Luntai (41.78°N, 84.25°E); Korla (41.75°N, 86.13°E); Kumishi (42.23°N, 88.22°E); Dabancheng (43.35°N, 88.32°E); Turpan (42.93°N, 89.2°E);
		Thirteen rooms (43.22°N, 91.73°E); Hami (42.82°N,93.52°E)
Southwest monsoon region	Tengchong	Tengchong (25.01°N,98.30°E,1648.7 m)

Sites	Sampling institutions	Analysis of institutions
(b)		
Zhangye	Key Laboratory of Eco Hydrology Inland River Basin, Chinese Academy of Science	Key Laboratory of Eco Hydrology Inland River Basin, Chinese Academy of Science
Lanzhou	The Northwest Normal University	The Geography and Environmental Science College, Northwest Normal University
Tianshan area	The national meteorological stations	The Physical Geography Laboratories, Northwest Normal University
Tengchong	The national meteorological stations	–
Nagqu	Nagqu Meteorological Station	The Laboratory of Ice Core and Cold Regions Environment, Cold and Arid Regions Environmental and Engineering Research Institute; Ecological Research Center of Kyoto University

Sites	Sampling period	Sample number	Analyses of the instrument	Measurement precision of $\delta^{18}O$	Measurement precision of δD	Data source
Zhangye	2013.10–2014.09	72 samples of rainfall	LGR, DLT-100	±0.3 ‰	±1 ‰	–
Lanzhou	2011.04–2013.02	420 of samples (with 49 samples of snow-only and 371 of Rain-only)	LGR, DLT-100	±0.2 ‰	±0.6 ‰	Chen et al. (2015)
Tianshan area	2012.08–2013.09	1052 of samples (with 208 samples of snow-only, 813 of Rain-only and 208 of sleet)	LGR, DLT-100	±0.2 ‰	±0.6 ‰	Wang (2015)
Tengchong	2009.01–2011.12	339 of samples	LGR, DLT-100	±0.2 ‰	±1 ‰	Li et al. (2013)
Nagqu	During 2000	198 of samples (rain, sleet, and snow)	MAT-252 mass spectrometer	±0.2 ‰	±0.5 ‰	Liu et al. (2008a, b)

* Lanzhou lies in the eage of the northwest arid region which having a similar characteristics with northwest arid region, so it shoule be placed in the northwest arid region area

from the equilibrium state of deuterium (Zhang et al. 2011). Furthermore, influenced by the water vapor condensation temperature, water vapor sources and its transmissions as well as seasonality of meteorological factors during precipitation, the slope and intercept of the local meteoric water line (LMWL) are usually different

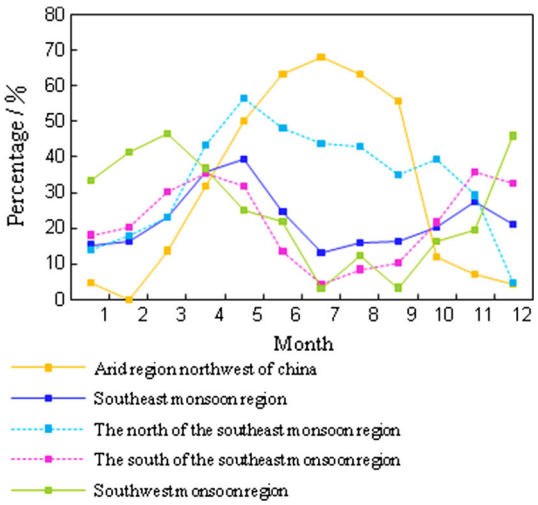

Fig. 2 Monthly value of the sample, which $\delta^{18}O$ is greater than average and d-excess is less than average, accounts for the proportion of the monthly total number of samples

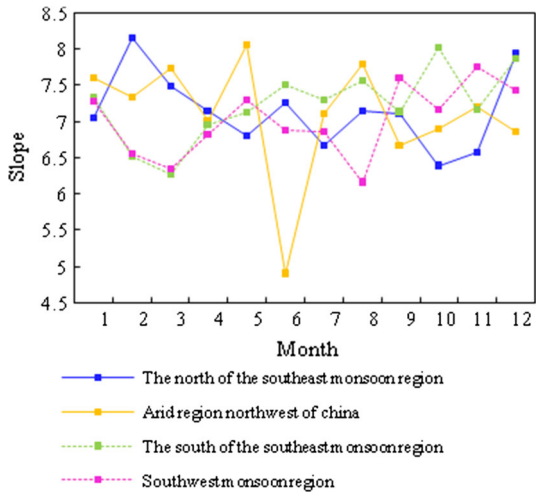

Fig. 3 Monthly variation of the slope in different regions

from GMWL (Meng and Liu 2010). The number of samples was calculated in the northwest arid region, southeast monsoon region, the southwest monsoon, and the Qinghai–Tibet Plateau in this study (Figs. 2 and 3). There are calculated data, which are greater than the average data in $\delta^{18}O$ and less than the average in d-excess is chosen to account for the proportion of the total monthly sample. At the same time, it, respectively, calculates the local meteoric water line equation under the monthly weighted average values and under the original data values of δD and $\delta^{18}O$, so as to explore and certify the existence of the sub-cloud secondary evaporation in different areas.

With the similar changes in the northwest arid region and the north of the southeast monsoon region, the samples whose $\delta^{18}O$ is greater than average and d-excess is less than average number accounting for the proportion of the total monthly sample show the high trend in summer and low trend in winter. In the northwest arid region, from January to July, it rises, while during August to December, it reduces gradually. The peak appears in summer and the lowest in winter (Fig. 2). The slope, intercept, and d-excess have a large variation and change the synchronization from May to August, showing the characteristics affected by the sub-cloud secondary evaporation. In June, the slope, intercept, and d-excess are the lowest, and the second evaporation is the most intense (Fig. 3). In addition, a weak synchronous rising trend from September to November can be discovered (Fig. 4a). This phenomenon is consistent with the study of Cheng in Lanzhou, which concluded that the estimated secondary evaporation rate was generally lower in winter and higher in summer (Chen et al. 2015). In the north of the southeast monsoon region, the samples rise from January to May and tend to be stable from May to November, and then they show a trend of decreasing after November. From February to June, the secondary evaporation effect is obvious, and the slope, intercept, and d-excess simultaneously reduce from February to May, making that sub-cloud secondary evaporation gradually become strong. From October to December, they rise synchronously. During this period, the secondary evaporation effect is weakened (Fig. 4b). In the south of the southeast monsoon region and southwest monsoon region, the samples have the same change (Fig. 2). They all indicate the regularity of high in winter and low in summer, which is in accordance with the seasonal change of δD and $\delta^{18}O$ in precipitation. The second evaporation effect of two areas has not obvious seasonal variation. During January to March, the secondary evaporation effect is slightly strengthened, What is more in the south of the southeast monsoon region, the slope, intercept, and d-excess are synchronous to change significantly from May to July and September to December, which showing that there are influences of the sub-cloud secondary evaporation. In addition to the rest of the month, there are no obvious changing rules. In Qinghai–Tibet Plateau the monsoon region, they transit gradually to the non-monsoon region from the south to the north. It is the arid local climate characteristics, making that the sub-cloud secondary evaporation of the raindrops become more intense in the process of landing from the south to the north (Yu et al. 2006, 2009; Zhang and Yao 1996; Tian et al. 2001). It follows that both in the northwest arid region and the north of the southeast monsoon region, seasonal variation of secondary evaporation is obvious, showing a strong variation in summer and weak variation in winter. In the northwest arid region, secondary evaporation gradually intensifies in late spring to early summer (May to June) and becomes strongest in June. In autumn (September to

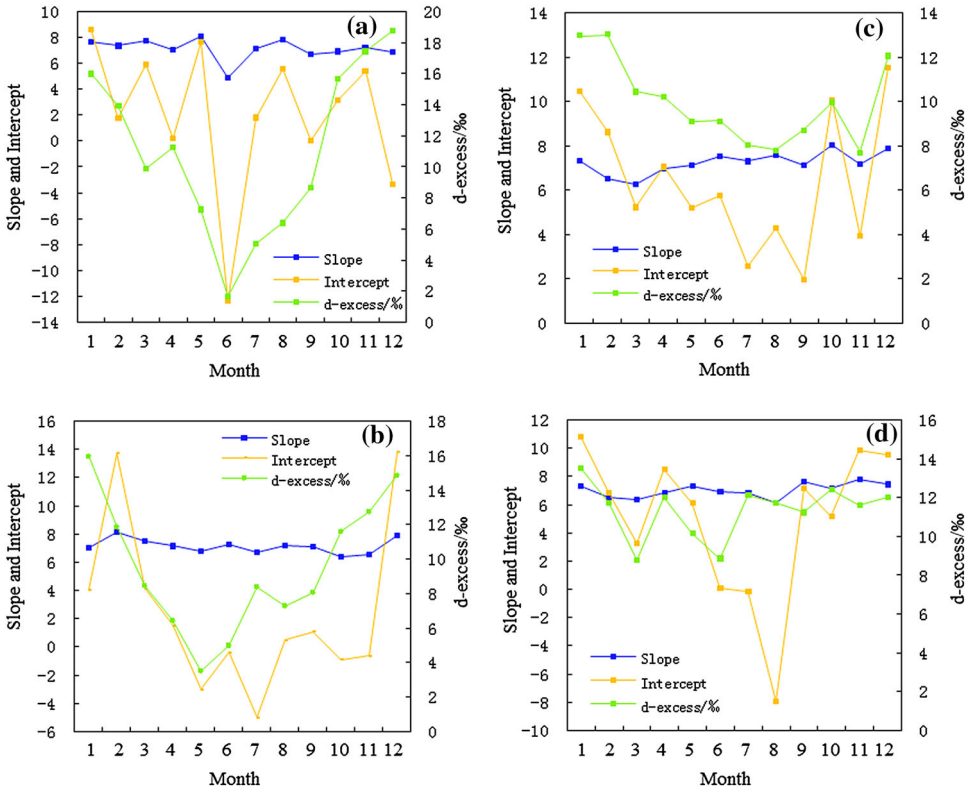

Fig. 4 Monthly variation of the slope, intercept, and d-excess in different regions [northwest arid region (**a**), the north of the southeast monsoon region (**b**), the south of the southeast monsoon region (**c**), the southwest monsoon region (**d**)]

November), the sub-cloud secondary evaporation gradually weakens. In the north of the southeast monsoon region, the secondary evaporation effect exists, and it gradually intensifies in late winter to spring (February to May) and weakens in autumn to early winter (October to December). On the contrary, in the south of the southeast monsoon region and southwest monsoon region, the seasonal change of second evaporation is not obvious, it is slightly heighten in late winter to early spring (January to February), and it has no obvious variation during the other months. In addition, the dominant factors that affect sub-cloud secondary evaporation in different areas may be different. In middle and high latitudes, especially in the high latitude inland area, temperature difference is large due to long-term influences of continental air mass in summer and winter, so we can conclude that it may be affected more by temperature in the northwest arid region, the north of the southeast monsoon region, and the northern Qinghai–Tibet Plateau. On the contrary, the monsoon climate significantly affected the middle and low latitude coastal areas and the southern region of the Qinghai Tibet Plateau: air mass from the ocean have high humidity, weak evaporation and abundant rainfall in summer while air carried by westerly circulation has the characteristics of continental air mass of low humidity, strong evaporation, and low rainfall in winter (Zhang and Yao 1998); therefore, we conclude that it is affected by relative humidity, precipitation, and seasonal alternation of different origin of air mass in the south of the southeast monsoon region, southwest monsoon region, and southern Qinghai–Tibet plateau.

Researching from the meteoric water line equation (Table 2), we can see that the slope and intercept from the original data are higher than those from the monthly precipitation weighted average value in the northwest arid region and the north of the southeast monsoon region, while the results are just acts opposite in the south of the southeast monsoon region and southwest monsoon region. This conclusion further verifies the differences between two types of regions. In addition to the Qinghai–Tibet Plateau lacks of data, the rest of the slope and intercept has the biggest value of snowfall in the sample. All samples of original data are greater than rainfall samples of original data, and the least is monthly weighted average from the slope and intercept in the northwest arid region and the north of the southeast monsoon region. The cause of this phenomenon may be related to a larger proportion of the regional snow events, which reduced the isotope fractionation in the process of precipitation caused by secondary evaporation. As the snow fell from the cloud to the ground, part sublimated directly from solid to gas. This process had little impact on the isotopic composition in snow, and the collected samples retained the isotopic characteristics within the clouds, namely, the sample of the snowfall has a higher slope, intercept, and d-excess. In the south of the

Table 2 Parameters of the local meteoric water line in different regions

Regions	Snow sample	Original data values	Rain sample	Monthly weighted average values
Northwest arid region				
Slope	7.310	7.208	7.025	7.018
Intercept	3.125	1.703	0.843	0.288
R^2	0.850	0.945	0.919	0.999
Snow sample > original data values > rain sample > monthly weighted average values				
The north of the southeast monsoon region				
Slope	8.217	7.134	6.658	6.136
Intercept	14.310	1.205	−2.168	−5.834
R^2	0.975	0.925	0.889	0.969
Snow sample > original data values > rain sample > monthly weighted average values				
The south of the southeast monsoon region				
Slope	8.817	7.842	7.841	8.330
Intercept	17.807	8.925	8.886	15.210
R^2	0.938	0.933	0.934	0.994
Snow sample > monthly weighted average values > original data values > rain sample				
Southwest monsoon region				
Slope	8.555	7.707	7.401	8.293
Intercept	23.784	9.133	6.765	14.310
R^2	0.972	0.929	0.912	0.997
Snow sample > monthly weighted average values > original data values > rain sample				

southeast monsoon region and southwest monsoon region, the slope and intercept of monthly weighted average value are greater than all samples of original data, and the least is rainfall samples, indicating that the proportion of rainfall events in the whole process of precipitation is extremely high, and during the landing of drops (especially small rainfall events), the slope and intercept decrease as a result of sub-cloud secondary evaporation.

Impact factors on secondary evaporation

The influence of precipitation

To analyze the influence of precipitation on secondary evaporation of regional atmospheric precipitation isotope, the samples are divided into two types, including the snow samples and the rain samples. The rain samples are divided into groups depending on the amount of rainfall for the separate relation analysis, respectively, of δD–$\delta^{18}O$ at each level of rainfall.

As shown in Fig. 5, in the northwest arid region, the slope, intercept, and d-excess have low values, and their synchronous changes can be obviously found when rainfall is less than 30 mm. In addition, the amount of rainfall over 30 mm can cause the phenomenon in which the d-excess becomes high and the changes in slope, intercept, and d-excess are relative disordered, showing that when the rainfall is less than 30 mm, the evaporation of raindrops is higher when they are dropping. There is no incremental change in the growth of slope, intercept, and d-excess on entire piecewise interval of rainfall. In addition, the segmentation of rainfall samples of 0–5 mm shows the strong secondary evaporation, indicating that in light rainfall, the kinetic fractionation strongly changes the isotopic composition of rainfall, which reduces the slope and intercept of regional precipitation. We also get the same conclusion according to the observation data in the northwest arid region (Table 3). With the rainfall decreased, d-excess value, the slope, and intercept of δD–$\delta^{18}O$ also decreased; meanwhile, the slope of the solid sample is larger than that of the liquid precipitation. The slope and intercept of the meteoric water line are the comprehensive effect of the condensing temperature, water vapor source and transmission path, and precipitation weather system factors (Merlivat and Jouzel 1979). The raindrops in the falling process experienced secondary evaporation, which produced the isotope fractionation effect. The slope and intercept of relatively large rainfall are closer to snow, suggesting that the snowfall isotopes are mainly for equilibrium fractionation process, and snow from the bottom of the cloud to the ground not change the ratio of isotopes. In light rainfall, the kinetic fractionation strongly changed the isotopic composition of rainfall, which reduced the slope and intercept of regional precipitation. In heavy rainfall and solid precipitation, the isotope fractionation effect was weaker, so that

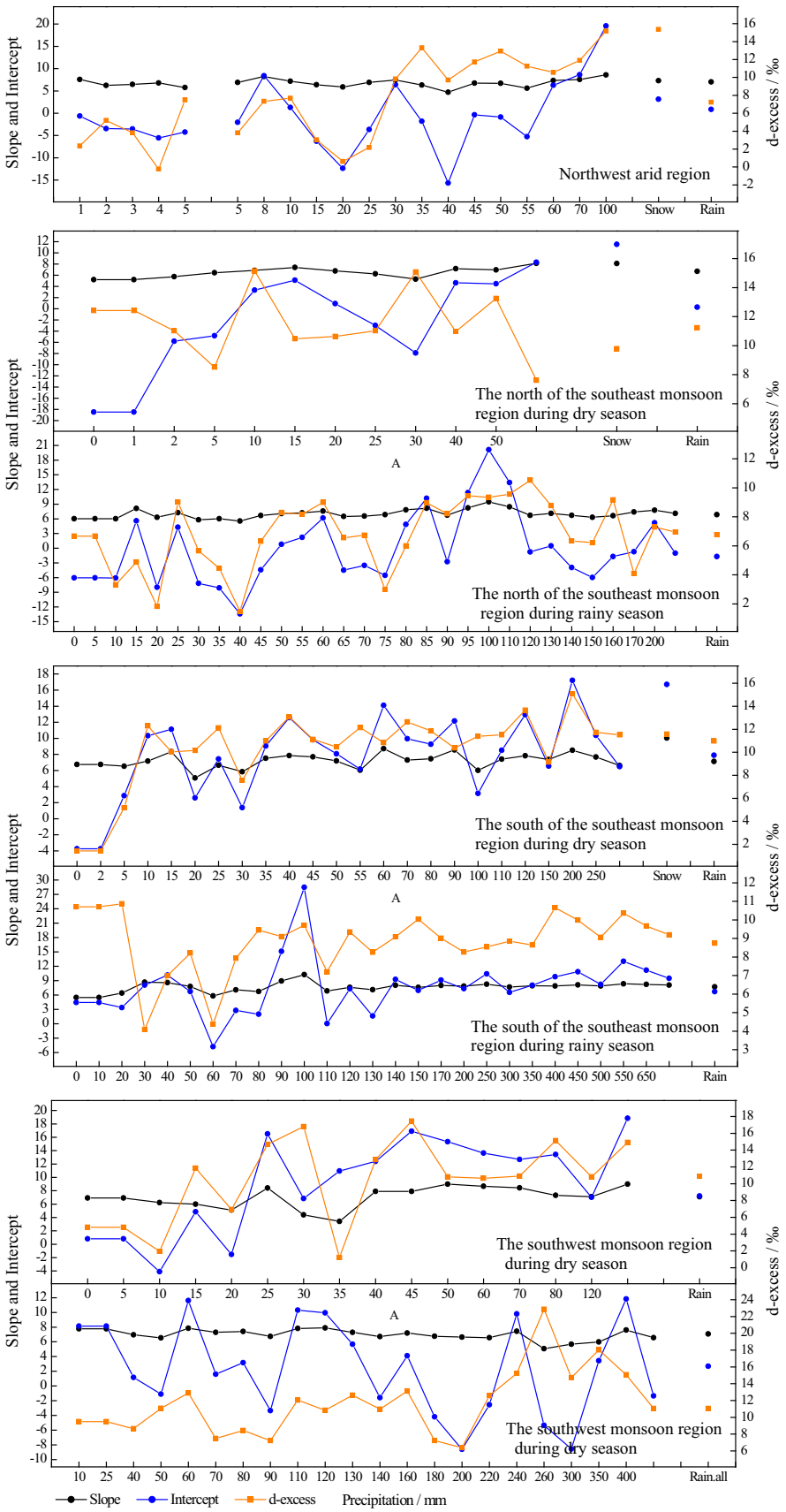

Fig. 5 Variation of the slope, intercept, and d-excess along with the change of precipitation in different regions. For samples which did not indicate the precipitation type, define the temperature in the northwest arid areas for snow samples under 2 °C, 2 °C or above for rainfall samples

Table 3 Observed data parameter values which isotopic characteristics affected by precipitation in some regions

Regions	Samples	Number of samples	d-excess/‰	δD–$\delta^{18}O$		
				Slope	Intercept/‰	R^2
Northwest arid region						
LanZhou	Total Samples	420	9.35	7.39	5.292	0.940
	Snow	49	11.11	8.02	11.286	0.962
	All	371	9.10	7.27	4.704	0.929
	$P > 15$ mm	17	13.54	7.8	11.446	0.977
	Rain					
	$5 < P \leq 15$ mm	66	12.27	7.8	10.776	0.948
	$2 < P \leq 5$ mm	85	9.69	7.49	6.498	0.920
	$1 < P \leq 2$ mm	72	9.14	7.32	5.319	0.933
	$0 < P \leq 1$ mm	131	6.50	7.1	2.239	0.915
Tianshan	Snow	208	9.0	7.94	6.31	0.97
	Sleet	31	12.1	7.70	6.93	0.98
	Rain					
	$P > 10$ mm	77	15.2	7.57	11.94	0.93
	2–10 mm	292	10.6	7.35	5.61	0.95
	1–2 mm	155	2.5	6.80	−2.05	0.91
	0.5–1 mm	127	−0.9	6.13	−5.54	0.91
	0.1–0.5 mm	162	−5.8	5.81	−10.23	0.89
ZhangYe	Rain					
	$P > 15$ mm	4	15.09	7.741	20.499	0.717
	$5 < P \leq 15$ mm	23	10.51	4.259	−12.737	0.425
	$2 < P \leq 5$ mm	17	7.42	7.176	−1.412	0.510
	$1 < P \leq 2$ mm	14	4.86	6.167	−3.865	0.628
	$0 < P \leq 1$ mm	14	4.25	4.185	−12.081	0.741
Southwest monsoon region						
TengChong	Rain					
	$50 \leq P < 100$ mm	6	–	8.48	16.28	0.99
	$25 \leq P < 50$ mm	32	–	8.37	15.98	0.99
	$10 \leq P < 25$ mm	105	–	8.23	12.83	0.99
	$P < 10$ mm	196	–	7.97	9.35	0.98
Nagqu	Rain					
	10–20 mm	3	17.3	7.4	6.6	0.99
	5–10 mm	17	12.9	7.7	6.6	0.99
	2–5 mm	36	14.3	8.0	14.1	0.99
	1–2 mm	31	13.2	7.9	11.4	0.98
	0–1 mm	60	5.8	7.3	−6.4	0.94

the slope and intercept were larger (Chen et al. 2015; Wang 2015).

Observed from different slopes, intercepts, and d-excess values in different seasons of the southeast monsoon region, the slope, intercept, and d-excess of the local meteoric water line equation from the south to the north are reduced overall, and the northern regions have the same variation during the period from dry season to rainy season, indicating that the secondary evaporation in northern regions is more intense than that in the southern regions. At the same time, the secondary evaporation in northern regions during rainy seasons is more intense than that during dry seasons. This is because the influence of temperature on sub-cloud secondary evaporation is greater than relative humidity and rainfall in these regions (Table 4).

When the amount of rainfall is less than 95 mm or more than 130 mm, there are obvious synchronous changes with the increase in rainfall that changes with tooth shape distribution on the slope, intercept, and d-excess in the north

Table 4 Parameters of the local meteoric water line in the north and south of the southeast monsoon region in different periods

	Slope	Intercept	d-excess	R2
The north region during rainy reason	6.861	−1.709	6.77	0.872
The north region during dry reason	7.324	4.603	11.22	0.943
The south region during rainy reason	7.700	6.713	8.74	0.930
The south region during dry reason	7.163	8.052	11.00	0.874

of the southeast monsoon region during the rainy seasons. There is secondary evaporation in this range; nevertheless, the slope, intercept, and d-excess do not show incremental changing trend with the increase in rainfall. This phenomenon also performs that rainfall is far from reaching saturation vapor pressure during the rainy seasons in the north of the southeast monsoon region. When the amount of rainfall is 95–130 mm, the slope, intercept, and d-excess are in high and variable disordering state; secondary evaporation is not obvious, which is suspected to be the result of many factors (such as local water vapor circulation, and so on). The dry seasons of the north of the southeast monsoon region are affected by continental air mass, and the main moisture sources lie in both the transportation of westerly and inland evaporation water vapor supplies, so its rainfall and air humidity relatively less. When the amount of rainfall is 0–10 mm, the slope and intercept are descent, and the secondary evaporation is intense. In addition to the slope of 5–10 mm, the intercept and d-excess show obvious synchronous change rule, and the slope, intercept, and d-excess are not synchronized changes. The reason is that local moisture evaporation supplies are enough to cover the secondary evaporation effect; at the same time, the high value during the entire process of rainfall also shows the rainfall comes from the surface water supplies where d-excess is higher.

When the amount of rainfall in the south of the southeast monsoon region during the rainy seasons is less than 70 mm, changes in the slope, intercept, and d-excess are relatively disordered. At this interval, d-excess shows sudden high and low values (possibly due to great effect on the maritime air masses intrusion at the early stage of the monsoon) (Yu et al. 2006, 2009). When the amount of rainfall is between 90 and 140 mm, these three factors change synchronously, showing a variation of tooth shape distribution. There is secondary evaporation at this stage, and the slope, intercept, and d-value do not present an increasing trend with the increase in rainfall. When rainfall is greater than 140 mm, the slope, intercept, and d-excess change fewer, with d-excess changing within about 10 ‰, slope almost unchanged, and is relatively close to slope of 8.0 of the GMWL, indicating that at this time, the rainfall is mainly marine vapor, virtually unaffected by sub-cloud secondary evaporation (Wang 2012), and isotopic composition of rainfall is similar to initial ocean water vapor. When rainfall is 0–20 and 50–100 mm in the south of the southeast monsoon region during the dry seasons, the slope, intercept, and d-excess change disorderly. When the rainfall reaches 20–50 mm or exceeds 100 mm, the slope, intercept, and d-excess all simultaneously change, and in 0–30 mm, the slope, intercept, and d-excess have more undervalued data. Except for 0–5 mm and individual points, d-excess at the range of other segments is greater than 10 ‰, indicating that except the sub-cloud secondary evaporation, the local moisture water supplies are also involved in the water cycle, secondary evaporation presents in all intervals of rainfall, and the slope, intercept and d-excess do not present an increasing trend with the increase of rainfall.

In the southwest monsoon region during rainy seasons, the slope, intercept, and d-excess simultaneously change clearly when its rainfall reaches 50–110 and 130–200 mm. In addition, when the d-excess is high after 200 mm with an average of 15.65, and the rainfall is less than 200 mm during rainy seasons, southwest monsoon region is affected by secondary evaporation, and the slope, intercept, and d-excess do not present an increasing trend with the increase in rainfall. The slope, intercept, and d-excess of dry season in southwest monsoon region show no obvious synchronous changes at all range of rainfall, only in sub-range of 15–25 mm, over 80 mm and individual intervals, they show synchronous changes, indicating that the southwest monsoon region during dry seasons has sub-cloud secondary evaporation at all precipitation intervals, and there is no relationship between rainfall and sub-cloud secondary evaporation. In addition to the secondary evaporation, local moisture supplies are also involved in the water cycle. When rainfall is 0–10 mm, the slope, intercept, and d-excess value are lower, indicating that small rainfall event in the region is affected by strong sub-cloud secondary evaporation. Most values of the slope, intercept, and d-excess of 10–40 mm are significantly lower than that when the rainfall exceeding 40 mm, showing that landing raindrops are influenced greater by secondary evaporation at the previous stage than that of the later stage. We found that the slope in Tengchong in rainy season is greater than dry season in observed data in the southwest monsoon region, while the intercept of rainy season is less than dry season, and this difference is not obvious. With the rainfall decreased, the slope and intercept of δD–$\delta^{18}O$ also decreased; meanwhile, the small rainfall

events are more strongly influenced by sub-cloud secondary evaporation in the landing process and have stronger isotope kinetic fractionation effect. In heavy rainfall, the isotope fractionation caused by sub-cloud secondary evaporation is relatively small (Li et al. 2013).

It is concluded that in the northwest arid region and the dry season of monsoon region, when rainfall is small, the slope, intercept, and d-excess of correlation equation of δD–$\delta^{18}O$ are relatively small, and they are strongly affected by sub-cloud secondary evaporation. Affected by continental climate, the air is dry in the northwest arid region and the dry season of monsoon region with low rainfall, and the precipitation almost comes from surface water vapor cycle, so in light rainfall, with the increasing of rainfall, evaporation becomes stronger, and the local moisture water supplies cover the sub-cloud secondary evaporation. During heavy rainfall, the slope and intercept change are relative disordered with higher d-excess, and sub-cloud secondary evaporation is weak at this moment. In addition to the larger or sustained rainfall conditions in the rainy season of monsoon region, where atmospheric moisture content is gradually close to saturated, the vapor pressure becomes larger, the secondary evaporation almost non-existent, and the slope and intercept of rainfall increase gradually and tend to be stable. At this time, the isotopic composition of rainfall is similar to the composition of the water vapor in the initial ocean. Except this period, between the intensity of rainfall and secondary evaporation, no relationship can be observed. By comparison, the observed data in every region show a better regularity. They all have common characteristics that with the rainfall decrease, the slope and intercept of δD–$\delta^{18}O$ also decrease. The small rainfall events are more strongly influenced by sub-cloud secondary evaporation in the landing process but in heavy rainfall, the isotope fractionation caused by sub-cloud secondary evaporation is relatively small (Meng and Liu 2010; Li et al. 2013; Chen et al. 2015; Wang 2015).

The influence of temperature

The collected rainfall isotope data are grouped according to the range of the temperature and analyze the correlation of δD–$\delta^{18}O$ at each sub-range (Fig. 6; Table 5).

When the temperature is less than 20 °C in the northwest arid region, the slope, intercept, and d-excess are higher and their synchronous changes are not obvious, and the characteristics of secondary evaporation are not strong. When the temperature exceeds 20 °C, the slope, intercept, and d-excess have almost low values with more slightly change. Under the circumstances that the range of temperature is between 23 and 30 °C, the slope, intercept, and d-excess change synchronously, showing a strong secondary evaporation effect within this range, but the phenomenon does not show the secondary evaporation strengthening significantly with temperature increasing, which may be affected by the mutual influence of other factors (Pang et al. 2011). According to measured data, the temperature had an effect on the secondary evaporation in Lanzhou city and surrounding area and in Tianshan, except when the temperature is less than 0 °C (snow events). With temperature increase, data above the freezing point showed a gradual decreasing trend in the d-excess value, slope, and intercept of the δD–$\delta^{18}O$ correlation equation (Chen et al. 2015; Wang 2015).

The slope, intercept, and d-excess synchronous changes are not obvious on entire piecewise interval of temperature during the dry season in the north of the southeast monsoon region, and the simultaneous changes appear only when temperature reaches −23 to −4 and −2 to 2 °C, and when the temperature exceeding 8 °C. When the temperature is less than 5 °C, the slope, intercept, and d-excess are relatively high, and the secondary evaporation is relatively weak; while the temperature exceeds 5 °C, the changes are opposite. Similarly, there is no more intense sub-cloud secondary evaporation with the increase in temperature within this range. In the north of the southeast monsoon region during the rainy season, when the temperature is in 8–14 and 19–24 °C, and some individual sub-ranges, the slope, intercept, and d-excess change synchronously. With the increase in temperature, the changes of the slope and intercept are relatively disordered. In addition, if over 20 °C, the d-excess is low.

The temperature is relatively high in the south of the southeast monsoon region during the dry season, basically above 0 °C. When the temperature reaches 1–11 °C, the slope, intercept, and d-excess reduce simultaneously with the temperature increasing. There is a good correlation relation between secondary evaporation and the temperature, and with the increase in the temperature, the sub-cloud secondary evaporation is gradually intense. When temperature is between 11 and 20 °C, the changes of the slope, intercept, and d-excess are relatively disordered, while in 20–24 °C, the slope, intercept, and d-excess change synchronously, showing a variation of tooth shape distribution, which indicates that there exists sub-cloud secondary evaporation in this stage. In the south of the southeast monsoon region during the rainy season, the slope, intercept, and d-excess are higher when temperature is less than 20 °C, and the slope and d-excess change fewer when temperature is greater than 20 °C, with slope basically remains at around 7.726 and d-excess remains at about 8.46.

In the southwest monsoon region during the dry season when temperature is in 3–8 °C, the slope, intercept, and d-excess are high, and the secondary evaporation is weak.

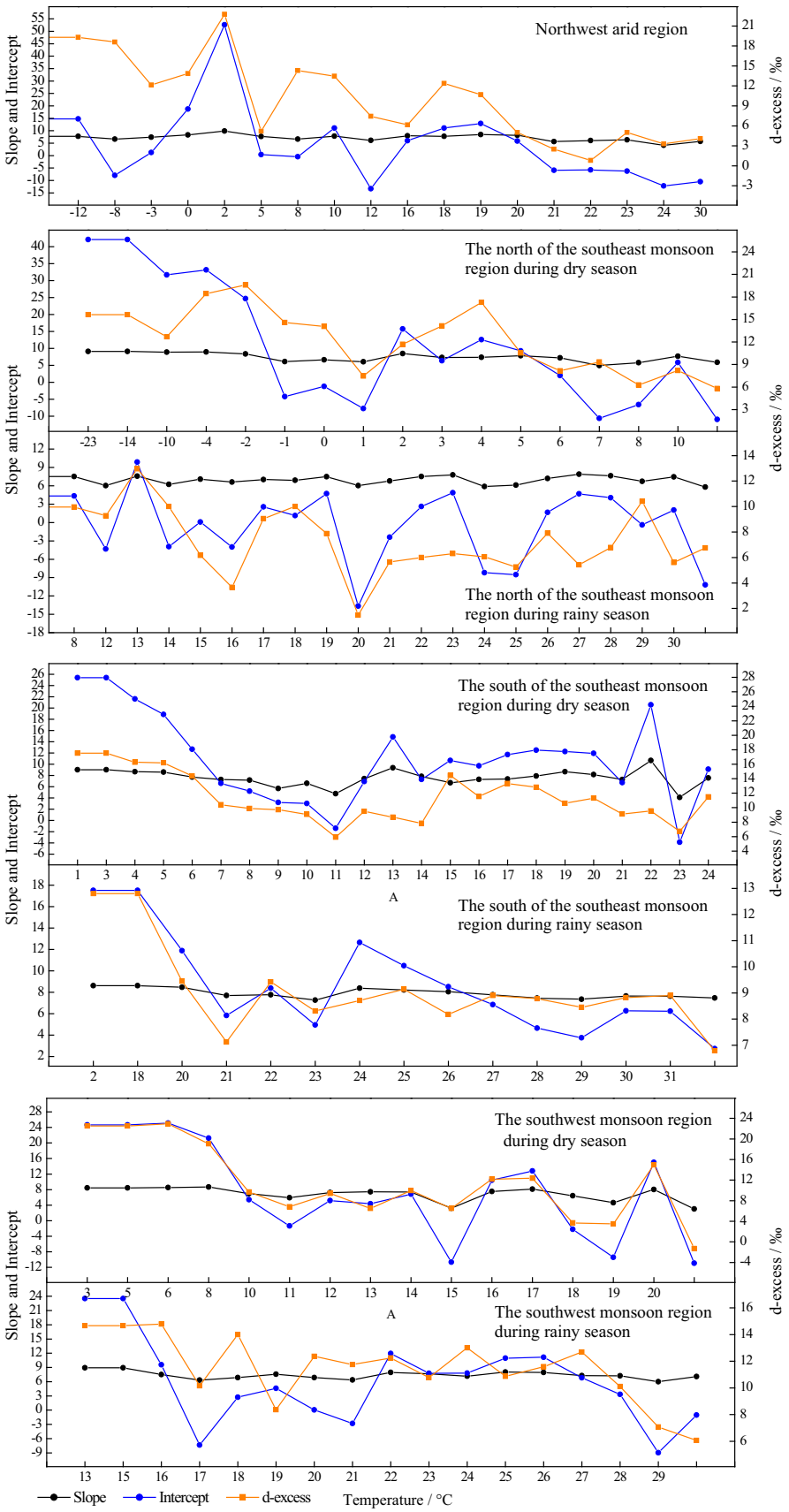

Fig. 6 Variation of the slope, intercept, and d-excess along with the change of temperature in different regions

Table 5 Observed data parameter values which isotopic characteristics affected by temperature in some regions

Regions	Temperature (°C)	Number of samples	d-excess (‰)	δD-δ^{18}O		
				Slope	Intercept (‰)	R^2
Northwest arid region						
LanZhou	$T \leq 0$	47	10.843	7.97	10.519	0.964
	$0 < T \leq 5$	18	17.569	7.61	14.913	0.926
	$5 < T \leq 10$	44	16.363	7.54	12.853	0.956
	$10 < T \leq 15$	103	10.584	7.64	8.379	0.962
	$15 < T \leq 20$	161	7.72	7.31	3.609	0.938
	$20 < T \leq 25$	40	1.409	6.99	−2.656	0.888
	$T > 25$	7	−0.745	6.94	−7.988	0.79
TianShan	$T < 0$	206	9.3	7.97	7.25	0.96
	$0 \leq T < 10$	183	14.7	7.52	6.20	0.96
	$10 \leq T < 20$	517	11.0	6.60	−0.46	0.88
	$T \geq 20$	146	−0.9	5.66	−8.27	0.87
ZhangYe	$T \leq 0$	8	9.24	6.18	−26.094	0.813
	$0 < T \leq 10$	11	8.94	5.122	−23.076	0.734
	$10 < T \leq 15$	9	12.04	8.827	22.149	0.516
	$15 < T \leq 20$	38	8.87	9.003	26.219	0.458
	$T > 20$	7	2.32	4.909	−21.855	0.523

In 8–14 °C, the slope, intercept, and d-excess change fewer, and the three factors all change synchronously in some sub-ranges, indicating the existence of sub-cloud secondary evaporation. Below 14 °C, the slope, intercept, and d-excess change synchronously and relatively large, while some values are low, indicating that sub-cloud secondary evaporation is relatively intense in this temperature range accompanied by other effects interacting (such as local moisture supply). The slope, intercept, and d-excess show a trend of synchronization in the southwest monsoon region during rainy season only in the individual interval of temperature (16–18, 20–23 °C). When the temperature is less than 28 °C, the d-excess is high and secondary evaporation effect exists, but it is relatively weak. When temperature is higher than 28 °C, there are all display low values with the strong secondary evaporation although the slope, intercept, and d-excess show no obvious synchronous changes.

It is concluded that apart from the north of the southeast monsoon region during rainy season, the secondary evaporation influenced by temperature has an acquirable regularity in the rest areas. In the northwest arid region, the dry season of the north of the southeast monsoon region, rainy season of the south of the southeast monsoon region and southwest monsoon region, the sub-cloud secondary evaporation is more intense in high temperature compared with low temperature, and the influence is not obvious in low temperature or there exists secondary evaporation, but its influence is quite weak. In the dry season in the south of the southeast monsoon region, the secondary evaporation shows a good correlation relation with temperature when the temperature is lower than 11 °C, and it gradually becomes more intense with the increase in temperature. In addition, the sub-cloud secondary evaporation is most intense with the value of the slope, intercept, and d-excess extremely low in 11 °C. When temperature exceeding 11 °C, the sub-cloud secondary evaporation shows the same phenomenon with the northwest arid region. The relationship between temperature and the slope of correlation equation of δD–δ^{18}O is not clear in the north of the southeast monsoon region during rainy season. Generally, the effect of temperature on the northwest arid region and the monsoon region in dry season is more than the monsoon rainy season, and on rainfall events, data are more than monthly average data. For rainfall events data, with temperature increase, the d-excess, slope and intercept of the δD–δ^{18}O gradually decrease, and sub-cloud secondary evaporation gradually increases in LanZhou and TianShan (Table 5).

The influence of atmospheric vapor pressure

Studies have shown that the atmospheric water vapor has less affect on the slope and intercept in snow samples and a greater impact on a small sample of rainfall (Meng and Liu, 2010). According to the difference of vapor pressure range, we have grouped the samples about snowfall, rainfall isotopic sample and less than 10 mm of rainfall, and analyzed the influence on slope and intercept in atmospheric waterline of the equation caused by vapor pressure.

Table 6 Biggest rangeability of the slope under the influence of vapor pressure in different regions

The biggest rangeability of the slope	Northwest arid region	The southeast monsoon region				The southwest monsoon region	
		The north of the region		The north of the region		Dry reason	Rainy reason
		Dry reason	Rainy reason	Dry reason	Rainy reason		
Rain sample	30.43	23.04	11.28	23.02	9.17	29.17	12.63
0–10 mm rain sample	58.73	116.09	40.03	35.39	–	129.11	–
Snow sample	12.33	18.72	–	–	–	–	–

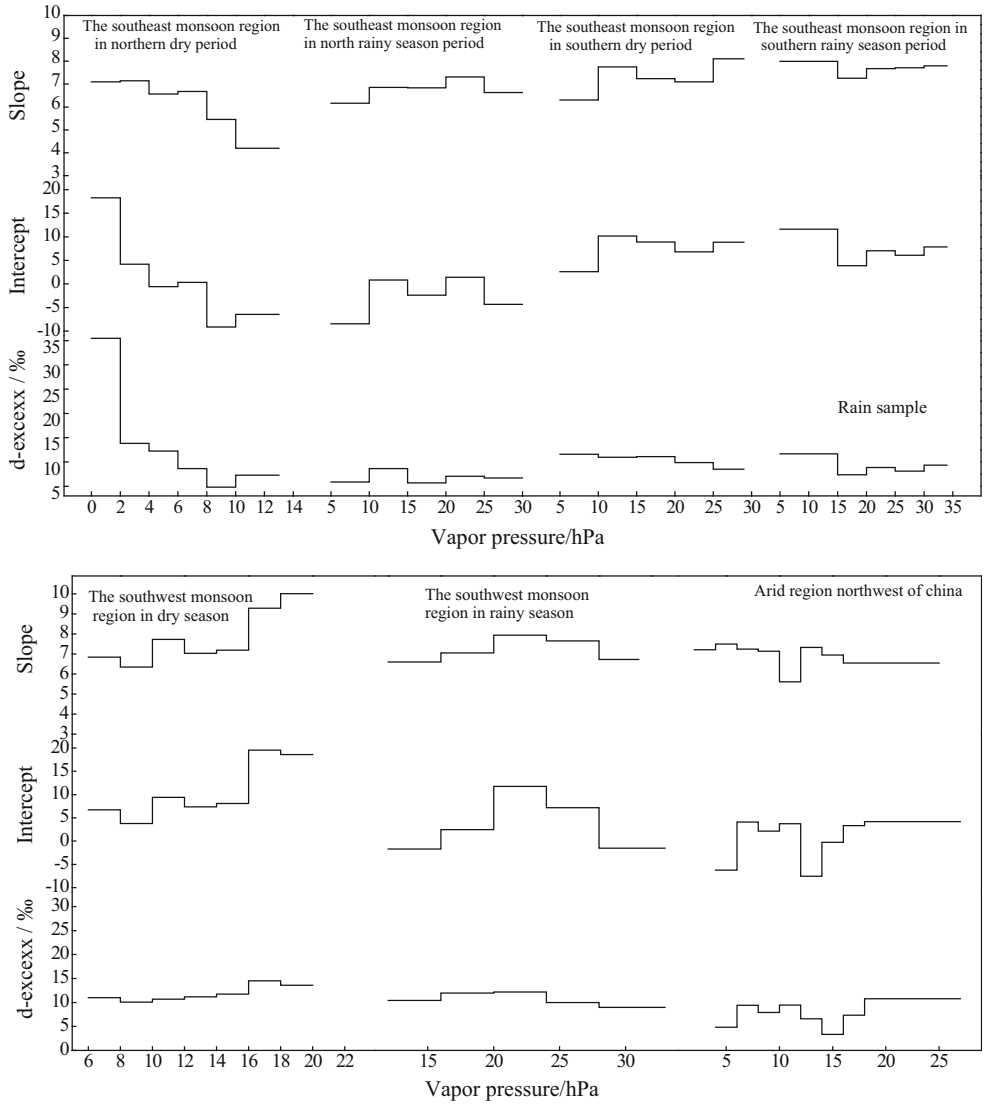

Fig. 7 Variation of the slope, intercept, and d-excess along with the change of vapor pressure in different regions

It can be concluded that a small change showed in the snow samples and a large change showed in rainfall range of 0–10 mm. The change of the slope, intercept, and d-excess affected by the vapor pressure in northwest arid region, and dry season of monsoon region is greater than that in rainy season (Table 6; Fig. 7), mainly because the air is dry in the northwest arid region and the dry season of monsoon region, which has lower moisture content and relative humidity influenced by continental air masses, as well as the vapor pressure is too far to reach the saturation condition, so the evaporation is intense. The reason why there are a fewer changes in snow samples is that some

Table 7 Biggest rangeability of the slope under the influence of humidity in different regions

The biggest rangeability of the slope	Northwest arid region	The southeast monsoon region				The southwest monsoon region	
		The north of the region		The north of the region		Dry reason	Rainy reason
		Dry reason	Rainy reason	Dry reason	Rainy reason		
Rain sample	7.2	37.41	4.83	6.04	9.98	12.63	8.09
0−10 mm rain sample	15.96	39	49	62.29	–	79.67	–
Snow sample	18	12.4	–	–	–	–	–

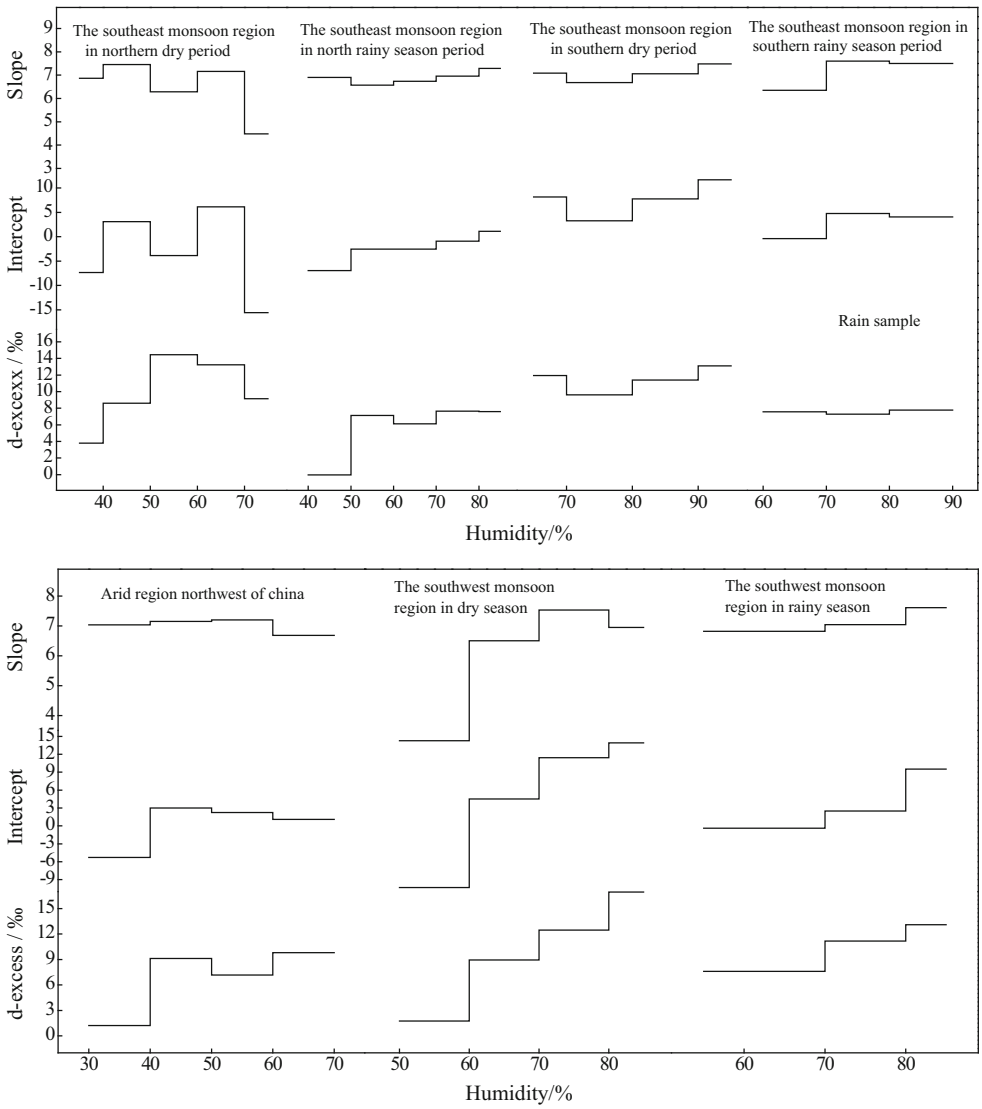

Fig. 8 Variation of the slope, intercept, and d-excess along with the change of humidity in different regions

snow changes from a solid directly into gas by sublimation as landing. The process has little effect on snow isotopic composition, and its isotope characteristics remain at the bottom of the clouds (δ^2H, $\delta^{18}O$, d-excess, etc.). Through the further analysis, we can find the facts that under the larger or sustained rainfall conditions, the atmospheric moisture content is gradually close to saturated, and vapor pressure becomes larger under the influence of vapor pressure change. At this time, the secondary evaporation becomes weaker and fractionation effect is also weakened caused by the imbalance of evaporation, leading to the slope and intercept increase and gradually stabilize (Meng and Liu 2010). In a word, the change of atmospheric water vapor pressure has little

effect on the slope, intercept, and d-excess of the snow samples, while they have larger influence on the rainfall samples. The effect of small rainfall events is the most intense. The relatively larger influences are in the northwest arid region and the dry season of the monsoon region, while the influences are tiny in the rainy season. This conclusion in the observed data has been further verified (Chen et al. 2015; Wang 2015).

The influence of relative humidity

The results show that in addition to the northwest arid region and the north of the southeast monsoon region during dry season, the rest of the slope, intercept, and d-excess in the area has significant regularity with the relative humidity change (Table 7; Fig. 8). When the relative humidity is more than 50 % in the southwest monsoon region in all season and the north of the southeast monsoon region during rainy season and more than 70 % in the south of the southeast monsoon region during dry season, the slope, intercept, and d-excess are showing a rising regularity with the relative humidity increasing. While the change of the slope is slight in this time and the maximum variation amplitude is 12.63, 8.09, 4.83, and 6.04 %, respectively. When the relative humidity is more than 70 % during the rainy season in the south of the southeast monsoon region, the changes of the slope, intercept, and d-excess are tiny, and the slope of the variation is 1.32 %. The above conclusion indicates that when the relative humidity is high, there is a good correlation relation between the relative humidity and the secondary evaporation. With the relative humidity increasing, water vapor pressure gradually tends to saturation, the slope, intercept, and d-excess of correlation equation of δD–$\delta^{18}O$ increase gradually and tend to be stable, and the sub-cloud secondary evaporation is gradually weakens. The extent of this impact is very weak, because the secondary evaporation at high relative humidity is the smaller. In the northwest arid region and the north of the southeast monsoon region during dry season, air is relatively dry and humidity is low, and the slope, intercept, and d-excess variable disorder. The maximum slope variation amplitude are 7.2 and 37.41 %, performing that when relative humidity is relatively low, its influence on slope, intercept, and d-excess is not obvious. In other words, in the northwest arid region and the north of the southeast monsoon region during the dry season, water vapor pressure is not sufficient to saturated state because of its low relative humidity, and the relative humidity has little influence on sub-cloud secondary evaporation during landing. Further study for the northwest arid region found that, when the relative humidity is high, with the increase in relative humidity, the slope, intercept, and d-excess have shown a sustained increase. Analyzing all monthly average samples of rainfall for 0–10 mm, we can observe that the slope, intercept, and d-excess change largely with no significant correlation relation between relative humidity, only showing rainfall has more intense sub-cloud secondary evaporation in this range, while the influence of relative humidity cannot be observed. For observed samples, the relative humidity had a small influence on the slope, intercept, and d-excess in snow. During light rainfall, the slope, intercept, and d-excess were greatly influenced by the relative humidity, and it increases with the increase in humidity tending to be the corresponding parameter values for snow samples.

Conclusions

1. Changes of the secondary evaporation effect are obvious in northwest arid areas and southeast monsoon region seasonal, strong in summer and weak in winter.
2. There is a strong secondary evaporation effect when rainfalls are less in both northwest arid areas and monsoon region in dry seasons. In addition, no relationship between the rainfall and the sub-cloud secondary evaporation can be observed.
3. Apart from the northern areas of southeast monsoon region during the rainy season, the evaporation effect at high temperature is more intense than that at low temperature in the rest areas. In northwest arid areas and in dry season of the northern areas of southeast monsoon region, the high temperature has stronger advantages than in rainy season of the south areas (southern southeast monsoon region and southwest monsoon region rainy season) and weakest in dry season of the southern region (southern southeast monsoon region and southwest monsoon region dry season). In addition to southeast monsoon region in the south during the dry season when the temperature is less than 11 °C, the secondary evaporation effect does not strengthen with the increasing temperature under other conditions.
4. The change of atmospheric water vapor pressure has little effect on the slope, intercept, and d-excess of the snow samples, while it has great influence on rainfalls. The impact on small rainfall events is the strongest. In addition, it affects northwest arid areas and monsoon season of drought more strongly, while it is opposite in rainy season.
5. In monsoon rainy season and the dry season of the south regions, when the relative humidity is high, the secondary evaporation effect weakens gradually with

the increasing of relative humidity, and there is no obvious correlation between secondary evaporation effect and relative humidity in northwest arid areas and southeast monsoon area during dry season in north.

Acknowledgments This research was funded by the Open-ended fund of State Key Laboratory of Cryosphere Sciences, Chinese Academy of Sciences (SKLCS-OP-2014-11), The Project of the northwest normal university young teachers scientific research ability promotion plan (NWNU-LKQN-13-10) and three Project of National Natural Science Foundation of China (41273010,41271133, 41461003), The project of major national research projects of China (2013CBA01808).

References

Araguás L, Froehlich K, Rozanski K. 1998. Stable isotope composition of precipitation over Southeast Asia[J]. J Geophys Res 103(28):721–728 **(742)**

Araguás L, Froehlich K, Rozanski K (2000) Deuterium and oxygen-18 isotope composition of precipitation and atmospheric moisture[J]. Hydrol Proc 14:1341–1355

Bowen GJ, Wilkinson B (2002) Spatial distribution of $\delta^{18}O$ in meteoric precipitation[J]. Geology 30:315–318

Chen FL, Zhang MJ, Wang SJ et al (2015) Relationship between subcloud secondary evaporation and stable isotopes in precipitation of Lanzhou and surrounding area[J]. Quatern Int 380–381(2015):68–74

Craig H (1961) Isotopic variations in meteoric waters[J]. Science 133:1702–1703

Dansgaard W (1953) The abundance of $\delta^{18}O$ in atmospheric water and water vapour[J]. Tellus 5(4):461–469

Dansgaard W (1964) Stable isotopes in precipitation[J]. Tellus 16(4):436–468

Friedman I, Redfield AC, Schoen B et al (1964) The variation of the deuterium content of natural waters in the hydrologic cycle[J]. Rev Geophys 2:1–124

Froehlich K, Kralik M, Papesch W et al (2008) Deuterium excess in precipitation of Alpine regions-Moisture recycling [J]. Isot Environ Health Stud 44(1):61–70

Gat JR (2000) Atmospheric water balance—the isotopic perspective[J]. Hydrol. Proc. 14:1357–1369

Gat JR, Matsui E (1991) Atmospheric water balance in the Amazon basin: an isotopic evapotranspiration model[J]. J Geophys Res 96:13179–13188

Gat JR, Bowser CJ, Kendall C (1994) The contribution of evaporation from the Great Lakes to the continental atmosphere: estimate based on stable isotope data[J]. Geophys Res Lett 21:557–560

Gourcy L, Groening M, Aggarwal PK (2005) Stable oxygen and hydrogen isotopes in precipitation. In: Aggarwal PK, Gat JR, Froehlich KFO (eds) Isotopes in the Water Cycle. Springer, Dordrecht, pp 39–51

Hoffman G, Jouzel J, Masson V (2000) Stable water isotopes in atmospheric general circulation models[J]. Hydrol Proc 14:1385–1406

Jouzel J, Merlivat L (1984) Deuterium and oxygen-18in precipitation: Modeling of the isotopic effect during snow formation[J]. J Geophys Res 89(D7):11749–11757

Kendall C, Coplen TB (2001) Distribution of oxygen-18 and deuterium in river waters across the United States[J]. Hydrol. Proc. 15:1363–1393

Kong YL, Pang ZH, Froehlich K (2013) Quantifying recycled moisture fraction in precipitation of an arid region using deuterium excess. Tellus B 65:19251. doi:10.3402/tellusb.v65i0.19251

Kress A, Saurer M, Siegwolf RTW, Frank DC, et al. 2010. A 350 years drought reconstruction from Alpine tree ring stable isotopes. Global Biogeochem Cycles 24:GB2011. doi:10.1029/2009GB003613

Kreutz KJ, Wake CP, Aizen VB et al (2003) Seasonal deuterium excess in a Tien Shan ice core:influence of moisture transport and recycling in Central Asia. Geophys Res Lett 30(18):1922. doi:10.1029/2003GL017896

Li G, Zhang XP, Zhang XZ et al (2013) Stable hydrogen and oxygen isotopes characteristics of atmospheric precipitation from Tengchong, YunNan[J]. Resour Environ Yangtze Basin 22(11):1458–1465

Liu ZF, Tian LD, Yao TD et al (2008a) Seasonal deuterium excess in Nagqu precipitation: influence of moisture transport and recycling in the middle of Tibetan Plateau [J]. Environ Geol 55:1501–1506

Liu Z, Tian L, Chai X et al (2008b) A model-based determination of spatial variation of precipitation $\delta^{18}O$ over China[J]. Chem Geol 249(1–2):203–212

Ma Q, Zhang MJ, Wang SJ et al (2012) Contributions of local moisture to precipitations in Western China[J]. Progress Geograph 31(11):1452–1459

Ma Q, Zhang MJ, Wang SJ et al (2013) Contributions of moisture from local evaporation to precipitations in Southeast China based on hydrogen and oxygen isotopes[J]. Progress Geograph 32(11):1712–1720

Ma Q, Zhang MJ, Wang SJ et al (2014) An investigation of moisture sources and secondary evaporation in Lanzhou, Northwest China. Environ Earth Sci 71(8):3375–3385

Meng YC, Liu GD (2010) Effect of below-cloud secondary evaporation on the stable isotopes inprecipitation over the Yangtze River basin[J]. Adv Water Sci 21(3):327–334

Merlivat L, Jouzel J (1979) Global climatic interpretation of the deuterium-oxygen 18 relationship for precipitation[J]. J Geophys Res 84(C8):5029–5033

Miyake Y, Matsubaya O, Nishihara C (1968) An isotopic study on meteoric precipitation. Papers Meteorol Geophys 19:243–266

Pang ZH, Kong YL, Froehlich K et al (2011) Processes affecting isotopes in precipitation of an arid region. Tellus 63B(3):352–359

Peng H, Mayer B, Harris S et al (2004) A 10-year record of stable isotope compositions of hydrogen and oxygen in precipitation at Calgary, Alberta, Canada. Tellus 56B:147–159

Peng H, Mayer B, Harris S et al (2007) The influence of below-cloud secondary effects on the stable isotope composition of hydrogen and oxygen in precipitation at Calgary, Alberta, Canada. Tellus 59B:698–704

Peng TR, Wang CH, Huang CC et al (2010) Stable isotopic characteristic of Taiwan's precipitation: a case study of western Pacific monsoon region[J]. Earth Planet Sci Lett 289:357–366

Rozanski K, Araguas L, Gonfiantini R (1993) Isotopic patterns in modern global precipitation. In: Swart PK, Lohmann KC, McKenzie J, Savin S (eds) Climate change in continental isotopic records, geophysics monograph No.78. American Geophysical Union, Washington, pp 1–36

Sengupta S, Sarkar A (2006) Stable isotope evidence of dual (Arabian Sea and Bay of Bengal) vapor sources in monsoonal precipitation over north India. Earth Planet Science Lett 250(3–4):511–521

Steen-Larsen HC, Masson-Delmotte V, Sjolte J et al (2011) Understanding the climatic signal in the water stable isotope records from the NEEM shallow firn/ice cores in northwest Greenland. J Geophys Res. doi:10.1029/2010JD014311

Stewart MK (1975) Stable isotope fractionation due to evaporation and isotopic exchange of falling water drops: applications to atmospheric processes and evaporation of lakes[J]. J Geophys Res 80(9):1133–1146

Tian LD, Yao TD, Sun WZ et al (2000) Study on stable isotope fractionation during water evaporation in the middle of the Tibetan Plateau. J Glaciol Geocryol 16(3):202–210

Tian LD, Yao TD, Song WZ (2001) The relationship of the precipitation between δD and $\delta^{18}O$ in the north and south Tibetan Plateau and water circulation. Sci China 31(3):214–220

Tian LD, Yao TD, MacClune K et al (2007) Stable isotopic variations in west China: a consideration of moisture sources. J Geophys Res 112(D10):D10112. doi:10.1029/2006JD007718

Wang T. 2012. The stable isotope temporal-spatial distribution of modern precipitation over east monsoon China and its implication for climate. Nan Jing: Nanjing University of Information Science and Technology, pp 1–63

Wang SJ (2015) Stable hydrogen and oxygen isotopes in precipitation of the Tianshan Mountains and their significance in hydrological cycle. Northwest Normal University, Lanzhou

Wang SP, Zhang CJ, Han YX (2010) Trend of potentia1evapotranspiration and pan evaporation and their main impact factors in different climate regions of Gansu province, J Desert Res 30(3):675–680

Yamanaka T, Tsujimura M, Oyunbaatar D et al (2007) Isotopic variation of precipitation over eastern Mongolia and its implication for the atmospheric water cycle[J]. J Hydrol 333(1):21–34

Yapp CJ (1982) A model for the relationship between precipitation D/H ratios and precipitation intensity. J Geophys Res 87(C12):9614–9620

Yu US, Tian LD, Ma YM et al (2006) Advances in the study of stable oxygen isotope in precipitation on the Tibetan Plateau[J]. Adv Earth Sci 21(12):1314–1323

Yu WS, Ma YM, Sun WZ et al (2009) Climatic significance of $\delta^{18}O$ records from precipitation on the western Tibetan Plateau. Chinese Sci Bull 54:2732–2741. doi:10.1007/s11434-009-0495-6

Yurtsever Y, Gat JR (1981) Atmospheric waters. In: Stable Isotope Hydrology: Deuterium and Oxygen-18 in the Water Cycle. Technical Report Series No. 210, International Atomic Energy Agency, Vienna, pp 103–142

Zhang XP, Yao TD (1994) World spatial characteristics of oxygen isotope ratio in precipitation. J Glaciol Geocryol 16(3):202–210

Zhang XP, Yao TD (1996) Relations between δD and $\delta^{18}O$ in precipitation at present in the Northeast Tibetan Plateau [J]. J Glaciol Geocryol 18(4):360–365

Zhang XP, Yao TD (1998) Distributional features of δ18O in precipitation in China[J]. Acta Geographica Sinica 53(4):356–364

Zhang XP, Xie ZC, Yao TD (1998) Mathematical modeling of variations on stable isotopic ratios in falling raindrops [J]. Acta Meteorologica Sinica 12(2):213–220

Zhang MJ, Ma Q, Li YJ et al (2011) Research of isotopic characteristic in precipitation and water vapor origin at the edge of monsoon region-A case study of Lanzhou city. J Northwest Normal Univ (Natural Sci Edit) 47(6):80–86

Zhang HT, Zhang ZH, Qian H (2012) Characteristics and influencing factors of hydrogen and oxygen isotopes in precipitation in Lanzhou. Int J Environ Eng Res 1:70–76